Nature of the Excited States of the Even-Even $^{98\text{-}108}$Ru Isotopes

Sohair M. Diab* and Salah A. Eid†

*Faculty of Education, Phys. Dept., Ain Shams University, Cairo, Egypt
†Faculty of Engineering, Phys. Dept., Ain Shams University, Cairo, Egypt
E-mail: mppe2@yahoo.co.uk

The positive and negative parity states of the even-even $^{98\text{-}108}$Ru isotopes are studied within the frame work of the interacting boson approximation model ($IBA-1$). The calculated levels energy, potential energy surfaces, $V(\beta,\gamma)$, and the electromagnetic transition probabilities, $B(E1)$ and $B(E2)$, show that ruthenium isotopes are transitional nuclei. Staggering effectle, $\Delta I = 1$, has been observed between the positive and negative parity states in some of ruthenium isotopes. The electric monopole strength, $X(E0/E2)$, has been calculated. All calculated values are compared with the available experimental and theoretical data wher reasonable agreement has obtained.

1 Introduction

The mass region $A = 100$ has been of considerable interst for nuclear structure studies as it shows many interesting features. These nuclei show back bending at high spin and shape transitions from vibrational to γ-soft and rotational characters. Many attempts have made to explore these structural changes which is due mainly to the n-p interactions.

Experimentally, the nuclear reaction ^{100}Mo (α, xn) [1] has been used in studying levels energy of ^{100}Ru. Angular distribution, γ-γ coincidences were measured, half life time has calculated and changes to the level scheme were proposed. Also, double beta decay rate of ^{100}Mo to the first excited 0^+ state of ^{100}Ru has measured experimentally [2] using γ-γ coincidence technique.

Doppler-shift attenuation measurements following the ^{100}Ru (n, $n`\gamma$) reaction [3] has used to measure the life times of the excited states in ^{100}Ru. Absolute transition rates were extracted and compared with the interacting boson model description. The 2^+(2240.8 keV) state which decays dominantly to the 2^+ via 1701 keV transition which is almost pure $M1$ in nature considered as a mixed-symmetry state. Again ^{100}Ru has been studied [4] experimently and several levels were seen where some new ones are detected below 3.2 MeV.

The excited states of ^{102}Ru have been investigated using ^{96}Zr (^{10}B, $p3n$) reaction [5] at a beam of energy 42 MeV and the emitted γ rays were detected.The analysis indicated that the nucleus is a γ-soft and the band crossing as well as staggering effect have observed.

Theoretically many models have been applied to ruthenium isotopes. Yukawa folded mean field [6] has applied to ^{100}Ru nucleus while the microscopic vibrational model has applied to ^{104}Ru and some other nuclei with their daughters [7]. The latter model was successful in describing the yrast 0^+ and 2^+ states of most of these nuclei and also some of their half-lives.

The very high-spin states of nuclei near A≈100 are investigated by the Cranked Strutinsky method [8] and many very extended shape minima are found in this region. Interacting boson model has been used in studying Ru isotopes using a $U(5)$–$O(6)$ transitional Hamiltonian with fixed parameters [9, 10] except for the boson number N. The potential arising from a coherent-state analysis indicate that ^{104}Ru is close to the critical point between spherical and γ-unstable structures.

Hartree-Fock Bogoliubov [11] wave functions have been tested by comparing the theoretically calculated results for ^{100}Mo and ^{100}Ru nuclei with the available experimental data. The yrast spectra , reduced $B(E2, 0^+ \to 2^+)$ transition probabilities, quadrupole moments $Q(2^+)$ and g factors, g(2^+) are computed. A reasonable agreement between the calculated and observed has obtained.

The microscopic anharmonic vibrator approach (MAVA) [12] has been used in investigating the low-lying collective states in $^{98\text{-}108}$Ru. Analysis for the level energies and electric quadrupole decays of the two-phonon type of states indicated that ^{100}Ru can interpreted as being a transitional nucleus between the spherical anharmonic vibrator ^{98}Ru and the quasirotational $^{102\text{-}106}$Ru isotopes.

A new emprical approach has proposed [13] which based on the connection between transition energies and spin. It allows one to distinguish vibrational from rotational characters in atomic nuclei. The cranked interacting boson model [14] has been used in estimating critical frequencies for the rotation-induced spherical-to-deformed shape transition in $A = 100$ nuclei. The predictions show an agreement with the back bending frequencies deduced from experimental yrast sequences in these nuclei.

The aim of the present work is to use the $IBA-1$ [15–17] for the following tasks:

(1) calculating the potential energy surfaces, $V(\beta,\gamma)$, to know the type of deformation exists;

(2) calculating levels energy, electromagnetic transition rates $B(E1)$ and $B(E2)$;

nucleus	EPS	$PAIR$	ELL	QQ	OCT	HEX	$E2SD(eb)$	$E2DD(eb)$
^{98}Ru	0.6280	0.000	0.0090	−0.0010	0.0000	0.0000	0.1250	−0.3698
^{100}Ru	0.5950	0.000	0.0085	−0.0200	0.0000	0.0000	0.1160	−0.3431
^{102}Ru	0.5650	0.0000	0.0085	−0.0200	0.0000	0.0000	0.1185	−0.3505
^{104}Ru	0.4830	0.0000	0.0085	−0.0200	0.0000	0.0000	0.1195	−0.3535
^{106}Ru	0.4560	0.0000	0.0085	−0.0200	0.0000	0.0000	0.1020	−0.3017
^{108}Ru	0.4540	0.0000	0.0085	−0.0200	0.0000	0.0000	0.1035	−0.3062

Table 1: Parameters used in IBA-1 Hamiltonian (all in MeV).

(3) studying the relation between the angular momentum I, the rotational angular frequency $\hbar\omega$ for bending in ruthenium isotopes;

(4) calculating staggering effect and beat patterns to detect any interactions between the (+ve) and (−ve) parity states; and

(5) calculating the electric monopole strength $X(E0/E2)$.

2 (IBA-1) model

2.1 Level energies

IBA-1 model was applied to the positive and negative parity states in even-even $^{98\text{-}108}$Ru isotopes. The Hamiltonian employed in the present calculation is:

$$\begin{aligned} H &= EPS \cdot n_d + PAIR \cdot (P \cdot P) \\ &+ \frac{1}{2} ELL \cdot (L \cdot L) + \frac{1}{2} QQ \cdot (Q \cdot Q) \\ &+ 5OCT \cdot (T_3 \cdot T_3) + 5HEX \cdot (T_4 \cdot T_4)\,, \end{aligned} \tag{1}$$

where

$$P \cdot p = \frac{1}{2} \left[\begin{array}{l} \left\{ (s^\dagger s^\dagger)_0^{(0)} - \sqrt{5}(d^\dagger d^\dagger)_0^{(0)} \right\} x \\ \left\{ (ss)_0^{(0)} - \sqrt{5}(\tilde{d}\tilde{d})_0^{(0)} \right\} \end{array} \right]_0^{(0)}, \tag{2}$$

$$L \cdot L = -10\sqrt{3} \left[(d^\dagger \tilde{d})^{(1)} x \, (d^\dagger \tilde{d})^{(1)} \right]_0^{(0)}, \tag{3}$$

$$Q \cdot Q = \sqrt{5} \left[\begin{array}{l} \left\{ (S^\dagger \tilde{d} + d^\dagger s)^{(2)} - \frac{\sqrt{7}}{2} (d^\dagger \tilde{d})^{(2)} \right\} x \\ \left\{ (s^\dagger \tilde{d} + +\tilde{d} s)^{(2)} - \frac{\sqrt{7}}{2} (d^\dagger \tilde{d})^{(2)} \right\} \end{array} \right]_0^{(0)}, \tag{4}$$

$$T_3 \cdot T_3 = -\sqrt{7} \left[(d^\dagger \tilde{d})^{(2)} x \, (d^\dagger \tilde{d})^{(2)} \right]_0^{(0)}, \tag{5}$$

$$T_4 \cdot T_4 = 3 \left[(d^\dagger \tilde{d})^{(4)} x \, (d^\dagger \tilde{d})^{(4)} \right]_0^{(0)}. \tag{6}$$

In the previous formulas, n_d is the number of boson; $P \cdot P$, $L \cdot L$, $Q \cdot Q$, $T_3 \cdot T_3$ and $T_4 \cdot T_4$ represent pairing, angular momentum, quadrupole, octupole and hexadecupole interactions between the bosons; EPS is the boson energy; and $PAIR$, ELL, QQ, OCT, HEX is the strengths of the pairing, angular momentum, quadrupole, octupole and hexadecupole interactions.

2.2 Transition rates

The electric quadrupole transition operator employed in this study is:

$$\begin{aligned} T^{(E2)} &= E2SD \cdot (s^\dagger \tilde{d} + d^\dagger s)^{(2)} + \\ &+ \frac{1}{\sqrt{5}} E2DD \cdot (d^\dagger \tilde{d})^{(2)}. \end{aligned} \tag{7}$$

The reduced electric quadrupole transition rates between $I_i \to I_f$ states are given by

$$B(E_2, I_i - I_f) = \frac{[< I_f \parallel T^{(E_2)} \parallel I_i >]^2}{2I_i + 1}. \tag{8}$$

3 Results and discussion

3.1 The potential energy surfaces

The potential energy surfaces [18], $V(\beta, \gamma)$, as a function of the deformation parameters β and γ are calculated using:

$$\begin{aligned} E_{N_\Pi N_\nu}(\beta, \gamma) &= \langle N_\pi N_\nu; \beta\gamma \, | H_{\pi\nu} | N_\pi N_\nu; \beta\gamma \rangle = \\ &= \zeta_d (N_\nu N_\pi) \beta^2 (1 + \beta^2) + \beta^2 (1 + \beta^2)^{-2} \times \\ &\times \left\{ k N_\nu N_\pi [4 - (\bar{X}_\pi \bar{X}_\nu) \beta \cos 3\gamma] \right\} + \\ &+ \left\{ [\bar{X}_\pi \bar{X}_\nu \beta^2] + N_\nu (N_\nu - 1) \left(\frac{1}{10} c_0 + \frac{1}{7} c_2 \right) \beta^2 \right\}, \end{aligned} \tag{9}$$

where

$$\bar{X}_\rho = \left(\frac{2}{7} \right)^{0.5} X_\rho \quad \rho = \pi \text{ or } \upsilon\,. \tag{10}$$

The calculated potential energy surfaces, $V(\beta, \gamma)$, are presented in Fig. 1. It shows that ^{98}Ru is a vibrational — like nucleus while $^{100-104}$Ru are γ-soft where the two wells on the oblate and prolate sides are equal. ^{106,108}Ru are rotational - like where they are prolate deformed.

I_i^+ I_f^+	^{98}Ru	^{100}Ru	^{102}Ru	^{104}Ru	^{106}Ru	^{108}Ru
0_1 Exp*. 2_1	0.392(12)	0.490(5)	0.630(10)	0.820(12)	0.770(20)	1.010(15)
0_1 Theor. 2_1	0.3930	0.4853	0.6279	0.8274	0.7737	1.0110
2_1 0_1	0.0786	0.0970	0.1256	0.1655	0.1547	0.2022
2_2 0_1	0.0000	0.0006	0.0012	0.0027	0.0032	0.0040
2_2 0_2	0.0226	0.0405	0.0548	0.0826	0.0870	0.1257
2_3 0_1	0.0000	0.0000	0.0000	0.0002	0.0006	0.0017
2_3 0_2	0.0658	0.0759	0.0993	0.1135	0.0853	0.0830
2_3 0_3	0.0093	0.0087	0.0121	0.0207	0.0264	0.0402
2_4 0_3	0.0041	0.0066	0.0121	0.0286	0.0448	0.0795
2_4 0_4	0.0565	0.0588	0.0712	0.0786	0.0530	0.0448
4_1 2_1	0.1260	0.1683	0.2257	0.3071	0.2912	0.3791
4_1 2_2	0.0092	0.0142	0.0190	0.0271	0.0267	0.0360
4_1 2_3	0.0269	0.0319	0.0424	0.0498	0.0384	0.0386
6_1 4_1	0.1420	0.2039	0.2838	0.3897	0.3681	0.4747
6_1 4_2	0.0172	0.0179	0.0228	0.0285	0.0256	0.0323
6_1 4_3	0.0208	0.0242	0.0333	0.0382	0.0292	0.0300
8_1 6_1	0.1264	0.2032	0.2998	0.4208	0.4012	0.5194
8_1 6_2	0.0247	0.0183	0.0223	0.0256	0.0217	0.0265
8_1 6_3	0.0113	0.0157	0.0239	0.0286	0.0228	0.0247
10_1 8_1	0.0791	0.1678	0.2768	0.4081	0.3997	0.5264
10_1 8_2	0.0319	0.0175	0.0207	0.0224	0.0183	0.0217

*Ref. 19.

Table 2: Values of the theoretical reduced transition probability, $B(E2)$ (in $e^2 b^2$).

I_i^+ I_f^+	^{98}Ru	^{100}Ru	^{102}Ru	^{104}Ru	^{106}Ru	^{108}Ru
1_1 0_1	0.0000	0.0030	0.0050	0.0104	0.0176	0.0261
1_1 0_2	0.1084	0.1280	0.1285	0.1280	0.1258	0.1227
3_1 2_1	0.1055	0.1211	0.1219	0.1306	0.1432	0.1564
3_1 2_2	0.0470	0.0415	0.0471	0.0544	0.0618	0.0712
3_1 2_3	0.0013	0.0002	0.0000	——	0.7737	——
3_2 2_1	0.0158	0.0024	0.0018	0.0029	0.0067	0.0130
3_2 2_2	0.0347	0.0197	0.0136	0.0102	0.0104	0.0121
3_2 2_3	0.1600	0.2126	0.2119	0.1943	0.1660	0.1352
5_1 4_1	0.2261	0.2533	0.2533	0.2605	0.2737	0.2881
5_1 4_2	0.0608	0.0480	0.0563	0.0648	0.0714	0.0784
5_1 4_3	0.0020	0.0006	——	——	0.7737	——
7_1 6_1	0.3657	0.3950	0.3912	0.3970	0.4083	0.4213
7_1 6_2	0.0609	0.0446	0.0551	0.0641	0.0701	0.0757
9_1 8_1	0.5276	0.5439	0.5367	0.5386	0.5465	0.5568
9_1 8_2	0.0425	0.0342	0.0472	0.0574	0.0640	0.0695
11_1 10_1	0.7143	0.6983	0.6872	0.6845	0.6882	0.6951

Table 3: Values of the theoretical reduced transition probability, $B(E1)$ (in $\mu\, e^2 b$).

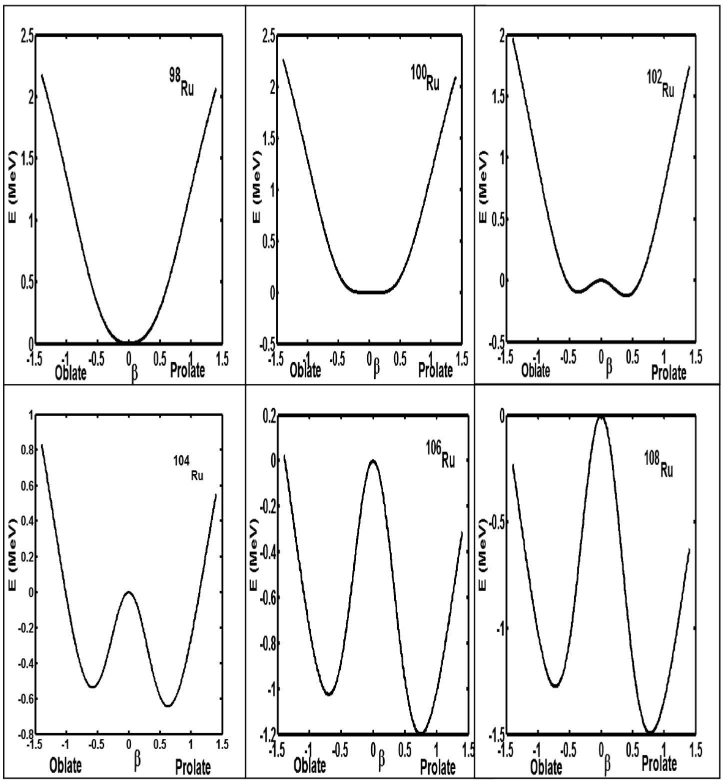

Fig. 1: Potential energy surfaces for $^{98\text{-}108}$Ru nuclei.

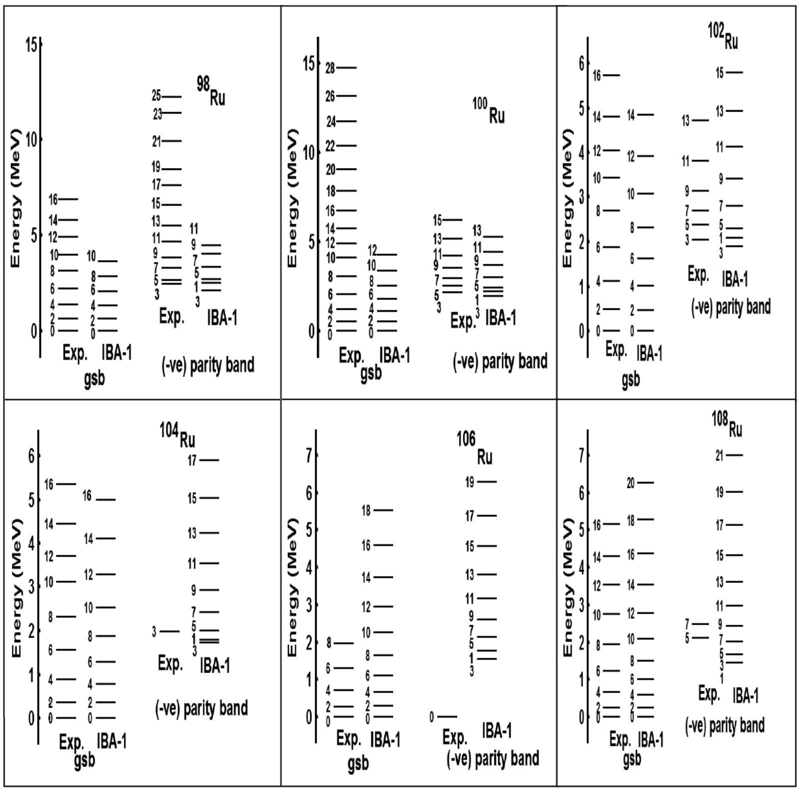

Fig. 2: Comparison between exp. [21–26] and theoretical (IBA-1) energy levels.

I_i^+	I_f^+	$I_{f}'^{+}$	^{98}Ru	^{100}Ru	^{102}Ru	^{104}Ru	^{106}Ru	^{108}Ru
0_2	0_1	2_1	0.011	0.027	0.057	0.166	0.213	0.227
0_3	0_1	2_1	0.250	0.347	1.333	0.894	1.076	1.328
0_3	0_1	2_2	0.001	0.009	0.005	0.010	0.086	0.112
0_3	0_1	2_3	1.000	0.042	0.026	0.024	0.043	0.130
0_3	0_2	2_1	—	0.086	0.500	0.421	0.184	0.171
0_3	0_2	2_2	—	0.002	0.002	0.004	0.014	0.014
0_3	0_2	2_3	—	0.010	0.010	0.011	0.007	0.016
0_4	0_1	2_2	1.600	0.010	0.046	—	—	—
0_4	0_1	2_3	0.024	0.010	0.003	—	—	—
0_4	0_1	2_4	0.363	0.113	0.003	—	—	—
0_4	0_2	2_2	1.200	0.030	0.097	—	—	—
0_4	0_2	2_3	0.018	0.034	0.070	0.114	0.476	0.808
0_4	0_2	2_4	0.272	0.340	0.142	1.035	3.696	2.082
0_4	0_3	2_1	0.111	0.454	—	—	0.558	0.458
0_4	0_3	2_2	0.600	0.010	0.010	—	0.002	0.611
0_4	0_3	2_3	0.009	0.011	0.007	—	0.074	0.058
0_4	0_3	2_4	0.136	0.113	0.015	—	0.575	0.150

Table 4. Theoretical $X_{if'f}\,(E0/E2)$ in Ru isotopes.

3.2 Energy spectra

The energy of the positive and negative parity states of ruthenium series of isotopes are calculated using computer code PHINT [20]. A comparison between the experimental spectra [21–26] and our calculations, using values of the model parameters given in Table 1 for the ground state band are illustrated in Fig. 2. The agreement between the calculated levels energy and their correspondence experimental values for all nuclei are slightly higher especially for the higher excited states. We believe this is due to the change of the projection of the angular momentum which is due mainly to band crossing.

Unfortunately there is no enough measurements of electromagnetic transition rates $B(E1)$ or $B(E2)$ for these series of nuclei. The only measured $B(E2, 0_1^+ \to 2_1^+)$'s are presented, in Table 2 for comparison with the calculated values. The parameters $E2SD$ and $E2DD$ are used in the computer code NPBEM [20] for calculating the electromagnetic transition rates after normalization to the available experimental values and displayed in Table 1.

No new parameters are introduced for calculating electromagnetic transition rates $B(E1)$ and $B(E2)$ of intraband and interband. Some of the calculated values are presented in Fig. 3 and show bending at $N = 60$, 62 which means there is an interaction between the $(+ve)$ and $(-ve)$ parity states of the ground state band.

The moment of inertia I and angular frequency $\hbar\omega$ are calculated using equations (11, 12):

$$\frac{2I}{\hbar^2} = \frac{4I-2}{\Delta E(I \to I-2)}\,, \tag{11}$$

$$(\hbar\omega)^2 = (I^2 - I + 1)\left[\frac{\Delta E(I \to I-2)}{(2I-1)}\right]^2. \tag{12}$$

The plots in Fig. 4 show back bending at angular momentum $I^+ = 10$ for $^{98\text{-}108}$Ru except ^{106}Ru where there is no experimental data available. It means, there is a crossing between the $(+ve)$ and $(-ve)$ parity states in the ground state band which confirmed by calculating staggering effect to these series of nuclei and the bending observed in Fig. 3.

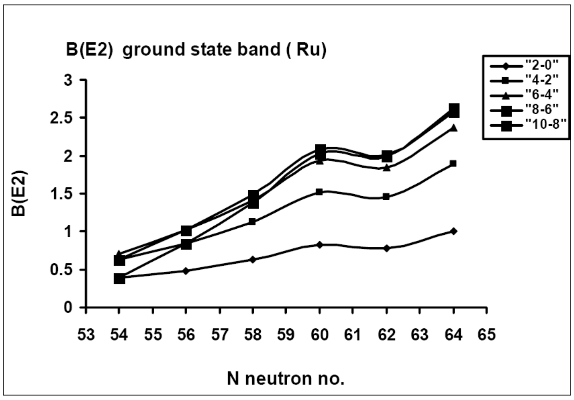

Fig. 3: The calculated $B(E2)$'s for the ground state band.

3.3 Electric monopole transitions

The electric monopole transitions, $E0$, are normally occurring between two states of the same spin and parity by transferring energy and zero unit of angular momentum. The strength of the electric monopole transition, $X_{if'f}\,(E0/E2)$, [27] can be calculated using equations (13, 14) and presented

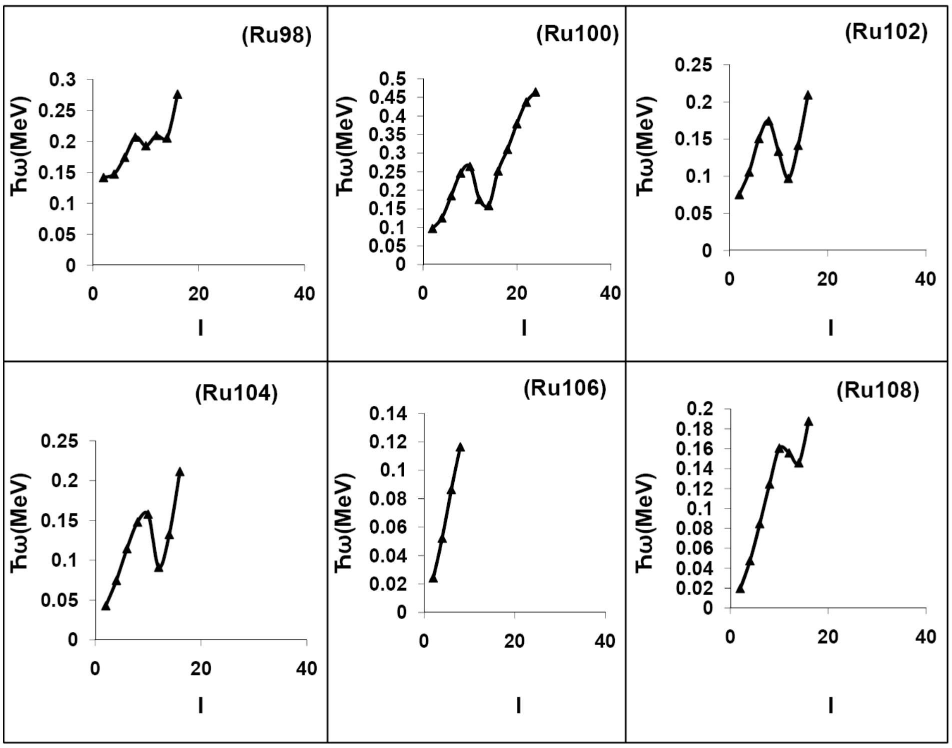

Fig. 4: Angular momentum I as a function of $(\hbar\omega)$.

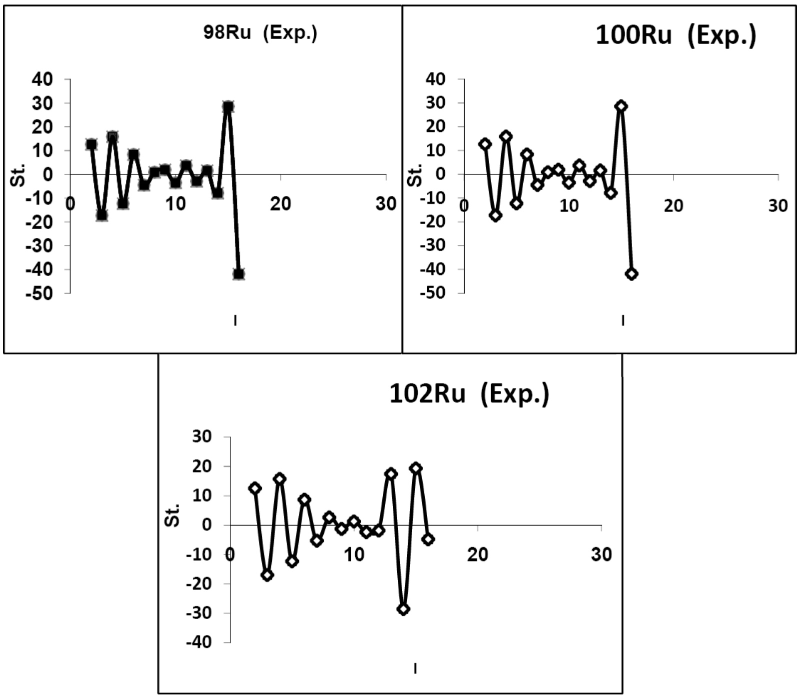

Fig. 5: $\Delta I = 1$, staggering patterns for $^{98\text{-}102}$Ru isotopes.

in Table 4

$$X_{if'f}(E0/E2) = \frac{B(E0, I_i - I_f)}{B(E2, I_i - I_{'f})}, \quad (13)$$

$$X_{if'f}(E0/E2) = (2.54\times10^9)\, A^{3/4} \times \\ \times \frac{E_\gamma^5(\text{MeV})}{\Omega_{KL}}\, \alpha(E2)\, \frac{T_e(E0, I_i - I_f)}{T_e(E_2, I_i - I_{'f})}. \quad (14)$$

3.4 The staggering

The presence of $(+ve)$ and $(-ve)$ parity states has encouraged us to study staggering effect [28–30] for $^{98\text{-}108}$Ru series of isotopes using staggering function equations (15, 16) with the help of the available experimental data [21–26].

$$Stag(I) = 6\Delta E(I) - 4\Delta E(I-1) - 4\Delta E(I+1) + \\ + \Delta E(I+2) + \Delta E(I-2), \quad (15)$$

with

$$\Delta E(I) = E(I+1) - E(I). \quad (16)$$

The calculated staggering patterns are illustrated in Fig. 5 and show an interaction between the $(+ve)$ and $(-ve)$ parity states for the ground state of $^{98\text{-}102}$Ru nuclei.

3.5 Conclusions

IBA-1 model has been applied successfully to $^{98\text{-}108}$Ru isotopes and we have got:

1. The levels energy are successfully reproduced;
2. The potential energy surfaces are calculated and show vibrational-like to ^{98}Ru, γ-soft to $^{100\text{-}104}$Ru and rotational characters to $^{106\text{-}108}$Ru isotopes where they are mainly prolate deformed nuclei;
3. Electromagnetic transition rates $B(E1)$ and $B(E2)$ are calculated;
4. Bending for $^{98\text{-}108}$Ru has been observed at angular momentum $I^+ = 10$ except for ^{106}Ru, where there is no experimental data are available;
5. Electromagnetic transition rates $B(E1)$ and $B(E2)$ are calculated;
6. Strength of the electric monopole transitions $X_{if'f}(E0/E2)$ are calculated; and
7. Staggering effect has been calculated and beat patterns are obtained which show an interaction between the $(-ve)$and $(+ve)$ parity states for $^{98\text{-}102}$Ru.

Submitted on August 23, 2008 / Accepted on August 29, 2008

References

1. Maazek J., Honusek M., Spalek A., Bielcik J., Slivova J. and Pasternak A. A. *Acta Physica Polonica B*, 1998, v. 29, 433.
2. Braeckeleer L. L., Hornish M., Barabash A. and Umatov V. *Phys. Rev.*, 2001, v. 86, 3510.
3. Genilloud L., Brown T. B., Corminboeuf F., Garrett P. E., Hannant C. D., Jolie J., Warr N. and Yates S. W. *Nucl. Phys. A*, 2001, v. 683, 287.
4. Horodynski-Matsushigue L. H., Rodrigues C. L., Sampaio F. C. and Lewin T. B. *Nucl. Phys. A*, 2002, v. 709, 73.
5. Lalkovski S. L., Rainovski G., Starosta K., Carpenter M. P., Fossan D. B., Finnigan S., Ilieva S., Joshi P., Koike T., Paul E. S., Pietralla N., Vaman C.and Wadsworth R. *Phys. Rev. C*, 2005, v. 71, 034318.
6. Nerlo-Pomorska B., Pomorski K. and Bartel J. *Phys. Rev. C*, 2006, v. 74, 034327.
7. Raina P. K. and Dhiman R. K. *Phys. Rev. C*, 2001, v. 64, 024310.
8. Chasman R. R.*Phys. Rev. C*, 2001, v. 64, 024311.
9. Frank A., Alonso C. E. and Arias J. M. *Phys. Rev. C*, 2001, v. 65, 014301.
10. Cejnar P., Jolie J. and Kern J. *Phys. Rev. C*, 2001, v. 63, 047304.
11. Chaturvedi K., Dixit B. M. and Rath P. K. *Phys. Rev. C*, 2003, v. 67, 064317.
12. Kotila J., Suhonen J. and Delion D. S. *Phys. Rev. C*, 2003, v. 68, 054322.
13. Regan P. H., Beausang C. W., Zamfir N. V., Casten R. F., Zhang J., Meyer D. A. and Ressler J. J. *Phys. Rev. Lett.*, 2003, v. 90 , 152502.
14. Cejnar P. and Jolie J. *Phys. Rev. C*, 2004, v. 69, 011301.
15. Arima A. and Iachello F. *Ann. Phys. (N.Y.)*, 1976, v. 99, 253.
16. Arima A. and Iachello F. *Ann. Phys. (N.Y.)*, 1978, v. 111, 201.
17. Arima A. and Iachello F. *Ann. Phys. (N.Y.)*, 1979, v. 123, 468.
18. Ginocchio J. N. and Kirson M. W. *Nucl. Phys. A*, 1980, v. 350, 31.
19. Raman S., de Nestor C. W., JR. and Tikkanen P. *Atomic Data and Nucl. Data Tab.*, 2001, v. 78, 128.
20. Scholten O. *The programm package PHINT (1980) version, internal report KVI-63, Gronigen: Keryfysisch Versneller Institut*.
21. Singh B. and Zhiqiang H. U *Nucl. Data Sheets*, 2003, v. 98, 335.
22. Singh B.*Nucl. Data Sheets*, 1997, v. 81, 1997.
23. Frenne D. D. and Jacobs E. *Nucl. Data Sheets*, 1998, v. 83, 535.
24. Blachot J. *Nucl. Data Sheets*, 1991, v. 64, 1.
25. Frenne D. D. and Jacobs E. *Nucl. Data Sheets*, 1994, v. 72, 1.
26. Blachot J. *Nucl. Data Sheets*, 2000, v. 91, 135.
27. Rasmussen J. O. Theory of $E0$ transitions of spheroidal nuclei. *Nucl. Phys.*, 1960, v. 19, 85.
28. Minkov N., Yotov P., Drenska S. and Scheid W. *J. Phys. G*, 2006, v. 32, 497.
29. Bonatsos D., Daskaloyannis C., Drenska S. B., Karoussos N., Minkov N., Raychev P. P. and Roussev R. P. *Phys. Rev. C*, 2000, v. 62, 024301.
30. Minkov N., Drenska S. B., Raychev P. P., Roussev R. P. and Bonatsos D. *Phys. Rev. C*, 2001, v. 63, 044305.